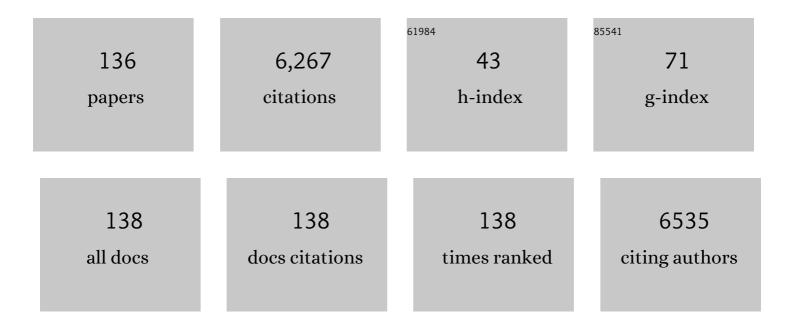
Yubo Luo

List of Publications by Year in descending order

Source: https://exaly.com/author-pdf/7556696/publications.pdf Version: 2024-02-01



VUROLUO

#	Article	IF	CITATIONS
1	Effects of La doping induced carrier concentration regulation and band structure modification on thermoelectric properties of PbSe. Scripta Materialia, 2022, 208, 114360.	5.2	12
2	High-performance and long-term thermal management material of MIL-101Cr@GO. Materials Today Physics, 2022, 22, 100572.	6.0	4
3	Cold-Sintered Bi ₂ Te ₃ -Based Materials for Engineering Nanograined Thermoelectrics. ACS Applied Energy Materials, 2022, 5, 2002-2010.	5.1	25
4	Thermoelectric Performance of the 2D Bi ₂ Si ₂ Te ₆ Semiconductor. Journal of the American Chemical Society, 2022, 144, 1445-1454.	13.7	37
5	ds-Block Element-Enabled Cooperative Regulation of Electrical and Thermal Transport for Extraordinary N- and P-Type PbSe Thermoelectrics near Room Temperature. Chemistry of Materials, 2022, 34, 1862-1874.	6.7	8
6	Extraordinary role of Zn in enhancing thermoelectric performance of Ga-doped n-type PbTe. Energy and Environmental Science, 2022, 15, 368-375.	30.8	107
7	Two-dimensional layered architecture constructing energy and phonon blocks for enhancing thermoelectric performance of InSb. Science China Materials, 2022, 65, 1353.	6.3	2
8	High-Performance Planar Perovskite Solar Cells with a Reduced Energy Barrier and Enhanced Charge Extraction via a Na ₂ WO ₄ -Modified SnO ₂ Electron Transport Layer. ACS Applied Materials & Interfaces, 2022, 14, 7962-7971.	8.0	17
9	High Thermoelectric Performance SnTe with a Segregated and Percolated Structure. ACS Applied Materials & Interfaces, 2022, , .	8.0	21
10	Electron Doping and Physical Properties in the Ferromagnetic Semimetal Co ₃ Sn _{2–<i>x</i>} Sb _{<i>x</i>} S ₂ . Journal of Physical Chemistry C, 2022, 126, 7230-7237.	3.1	1
11	Valence Disproportionation of GeS in the PbS Matrix Forms Pb ₅ Ge ₅ S ₁₂ Inclusions with Conduction Band Alignment Leading to High n-Type Thermoelectric Performance. Journal of the American Chemical Society, 2022, 144, 7402-7413.	13.7	24
12	Enhanced thermoelectric performance of orientated and defected SnTe. Journal of Alloys and Compounds, 2021, 858, 157634.	5.5	7
13	Strong Valence Band Convergence to Enhance Thermoelectric Performance in PbSe with Two Chemically Independent Controls. Angewandte Chemie, 2021, 133, 272-277.	2.0	7
14	Strong Valence Band Convergence to Enhance Thermoelectric Performance in PbSe with Two Chemically Independent Controls. Angewandte Chemie - International Edition, 2021, 60, 268-273.	13.8	28
15	Local Distortions and Metal–Semiconductor–Metal Transition in Quasi-One-Dimensional Nanowire Compounds AV ₃ Q ₃ O _{Î′} (A = K, Rb, Cs and Q = Se, Te). Chemistry of Materials, 2021, 33, 2611-2623.	6.7	6
16	Improving the Photovoltaic Performance of Flexible Solar Cells with Semitransparent Inorganic Perovskite Active Layers by Interface Engineering. ACS Applied Materials & Interfaces, 2021, 13, 20034-20042.	8.0	13
17	High Entropy Semiconductor AgMnGeSbTe ₄ with Desirable Thermoelectric Performance. Advanced Functional Materials, 2021, 31, 2103197.	14.9	50
18	Accelerated discovery of a large family of quaternary chalcogenides with very low lattice thermal conductivity. Npj Computational Materials, 2021, 7, .	8.7	32

#	Article	IF	CITATIONS
19	Band Matching Strategy for All-Inorganic Cs ₂ AgBiBr ₆ Double Perovskite Solar Cells with High Photovoltage. ACS Applied Materials & Interfaces, 2021, 13, 37027-37034.	8.0	36
20	High thermoelectric performance enabled by convergence of nested conduction bands in Pb7Bi4Se13 with low thermal conductivity. Nature Communications, 2021, 12, 4793.	12.8	53
21	Cubic AgMnSbTe ₃ Semiconductor with a High Thermoelectric Performance. Journal of the American Chemical Society, 2021, 143, 13990-13998.	13.7	56
22	Defect engineering in thermoelectric materials: what have we learned?. Chemical Society Reviews, 2021, 50, 9022-9054.	38.1	201
23	High Power Factor and Thermoelectric Figure of Merit in Sb ₂ Si ₂ Te ₆ through Synergetic Effect of Ca Doping. Chemistry of Materials, 2021, 33, 8097-8105.	6.7	21
24	High Thermoelectric Performance through Crystal Symmetry Enhancement in Triply Doped Diamondoid Compound Cu ₂ SnSe ₃ . Advanced Energy Materials, 2021, 11, 2100661.	19.5	39
25	Highâ€Efficiency and Durable Inverted Perovskite Solar Cells with Thermallyâ€Induced Phaseâ€Change Electron Extraction Layer. Advanced Energy Materials, 2021, 11, 2102844.	19.5	35
26	Tactfully decoupling interdependent electrical parameters via interstitial defects for SnTe thermoelectrics. Nano Energy, 2020, 67, 104292.	16.0	33
27	Improvement of photovoltaic performance of perovskite solar cells by interface modification with CaTiO3. Journal of Power Sources, 2020, 449, 227504.	7.8	16
28	High-Performance Thermoelectrics from Cellular Nanostructured Sb2Si2Te6. Joule, 2020, 4, 159-175.	24.0	103
29	Ecofriendly Highly Robust Ag ₈ SiSe ₆ -Based Thermoelectric Composites with Excellent Performance Near Room Temperature. ACS Applied Materials & Interfaces, 2020, 12, 54653-54661.	8.0	18
30	High Thermoelectric Performance in the New Cubic Semiconductor AgSnSbSe ₃ by High-Entropy Engineering. Journal of the American Chemical Society, 2020, 142, 15187-15198.	13.7	108
31	Ultralow Thermal Conductivity and Thermoelectric Properties of Rb2Bi8Se13. Chemistry of Materials, 2020, 32, 3561-3569.	6.7	23
32	Recent advances, design guidelines, and prospects of flexible organic/inorganic thermoelectric composites. Materials Advances, 2020, 1, 1038-1054.	5.4	37
33	High Thermoelectric Performance in SnTe Nanocomposites with All-Scale Hierarchical Structures. ACS Applied Materials & Interfaces, 2020, 12, 23102-23109.	8.0	47
34	In Situ Reaction Induced Core–Shell Structure to Ultralow κ _{lat} and High Thermoelectric Performance of SnTe. Advanced Science, 2020, 7, 1903493.	11.2	38
35	All-scale Architecturing of Microstructure in Chalcogenide Thermoelectric Materials. Microscopy and Microanalysis, 2019, 25, 2236-2237.	0.4	1
36	Synergistical Tuning Interface Barrier and Phonon Propagation in Au–Sb ₂ Te ₃ Nanoplate for Boosting Thermoelectric Performance. Journal of Physical Chemistry Letters, 2019, 10, 4903-4909.	4.6	26

#	Article	IF	CITATIONS
37	All-Inorganic CsPbBr ₃ Perovskite Solar Cells with 10.45% Efficiency by Evaporation-Assisted Deposition and Setting Intermediate Energy Levels. ACS Applied Materials & Interfaces, 2019, 11, 29746-29752.	8.0	126
38	Interfacing Epitaxial Dinickel Phosphide to 2D Nickel Thiophosphate Nanosheets for Boosting Electrocatalytic Water Splitting. ACS Nano, 2019, 13, 7975-7984.	14.6	171
39	High Figure of Merit in Gallium-Doped Nanostructured n-Type PbTe- <i>x</i> GeTe with Midgap States. Journal of the American Chemical Society, 2019, 141, 16169-16177.	13.7	76
40	Tuning the Thermoelectric Performance of SnTe via Dual-Site Electronic Donation and Super-Saturation Solution. ACS Applied Energy Materials, 2019, 2, 7490-7496.	5.1	11
41	Significant average <i>ZT</i> enhancement in Cu ₃ SbSe ₄ -based thermoelectric material <i>via</i> softening p–d hybridization. Journal of Materials Chemistry A, 2019, 7, 17648-17654.	10.3	41
42	Facile Route to High-Performance SnTe-Based Thermoelectric Materials: Synergistic Regulation of Electrical and Thermal Transport by In Situ Chemical Reactions. Chemistry of Materials, 2019, 31, 3491-3497.	6.7	31
43	Enhancement of Thermoelectric Performance for n-Type PbS through Synergy of Gap State and Fermi Level Pinning. Journal of the American Chemical Society, 2019, 141, 6403-6412.	13.7	67
44	Synergy of Nb Doping and Surface Alloy Enhanced on Water–Alkali Electrocatalytic Hydrogen Generation Performance in Tiâ€Based MXene. Advanced Science, 2019, 6, 1900116.	11.2	97
45	Tailoring the Carrier and Phonon Scattering to Enhanced Thermoelectric Performance of SnTe by Cation–Anion Codoping with Eco-Benign Cal2. ACS Applied Energy Materials, 2019, 2, 1997-2003.	5.1	25
46	High-Performance Flexible Perovskite Solar Cells with a Metal Sulfide Electron Transport Layer of SnS ₂ by Room-Temperature Vacuum Deposition. ACS Applied Energy Materials, 2019, 2, 382-388.	5.1	33
47	High Thermoelectric Performance in Polycrystalline SnSe Via Dualâ€Doping with Ag/Na and Nanostructuring With Ag ₈ SnSe ₆ . Advanced Energy Materials, 2019, 9, 1803072.	19.5	98
48	Effect of Sn doping on thermoelectric properties of p-type manganese telluride. Journal of Alloys and Compounds, 2019, 777, 968-973.	5.5	15
49	Enhancement of photovoltaic performance and moisture stability of perovskite solar cells by modification of tin phthalocyanine (SnPc). Electrochimica Acta, 2019, 296, 799-805.	5.2	12
50	Reinforced bond covalency and multiscale hierarchical architecture to high performance eco-friendly MnTe-based thermoelectric materials. Nano Energy, 2019, 57, 703-710.	16.0	28
51	Thermoelectric Performance of Rapidly Microwave-Synthesized α-MgAgSb with SnTe Nanoinclusions. Chemistry of Materials, 2019, 31, 2421-2430.	6.7	26
52	Enhanced thermoelectric performance of SnTe: High efficient cation - anion Co-doping, hierarchical microstructure and electro-acoustic decoupling. Nano Energy, 2018, 47, 81-88.	16.0	67
53	Achieving highly efficient electrocatalytic oxygen evolution with ultrathin 2D Fe-doped nickel thiophosphate nanosheets. Nano Energy, 2018, 47, 257-265.	16.0	122
54	Enhancement of photovoltaic performance of flexible perovskite solar cells by means of ionic liquid interface modification in a low temperature all solution process. Applied Surface Science, 2018, 440, 1116-1122.	6.1	36

#	Article	IF	CITATIONS
55	Improved densification and thermoelectric performance of In5SnSbO12 via Ga doping. Journal of Materials Science, 2018, 53, 6741-6751.	3.7	2
56	Enhancement of the thermoelectric performance of CulnTe2 via SnO2 in situ replacement. Journal of Materials Science: Materials in Electronics, 2018, 29, 4732-4737.	2.2	4
57	The improvement of thermoelectric property of bulk ZnO via ZnS addition: Influence of intrinsic defects. Ceramics International, 2018, 44, 6461-6465.	4.8	20
58	Low temperature processed ternary oxide as an electron transport layer for efficient and stable perovskite solar cells. Electrochimica Acta, 2018, 261, 474-481.	5.2	23
59	nâ€Type SnSe ₂ Orientedâ€Nanoplateâ€Based Pellets for High Thermoelectric Performance. Advanced Energy Materials, 2018, 8, 1702167.	19.5	103
60	Electrochemical deposition of PbI2 for perovskite solar cells. Solar Energy, 2018, 159, 300-305.	6.1	21
61	Simultaneous regulation of electrical and thermal transport properties in MnTe chalcogenides <i>via</i> the incorporation of p-type Sb ₂ Te ₃ . Journal of Materials Chemistry A, 2018, 6, 23473-23477.	10.3	23
62	Thermoelectric Performance: Enhancement of Thermoelectric Performance in CuSbSe 2 Nanoplateâ€Based Pellets by Texture Engineering and Carrier Concentration Optimization (Small) Tj ETQq0 0 0	rg₿īīq ́.O vei	lock 10 Tf 50
63	Asymmetric-Layered Tin Thiophosphate: An Emerging 2D Ternary Anode for High-Performance Sodium Ion Full Cell. ACS Nano, 2018, 12, 12902-12911.	14.6	45
64	Porous MXene Frameworks Support Pyrite Nanodots toward High-Rate Pseudocapacitive Li/Na-Ion Storage. ACS Applied Materials & Interfaces, 2018, 10, 33779-33784.	8.0	61
65	Enhancement of Thermoelectric Performance in CuSbSe ₂ Nanoplateâ€Based Pellets by Texture Engineering and Carrier Concentration Optimization. Small, 2018, 14, e1803092.	10.0	17
66	Mosaicâ€Structured Cobalt Nickel Thiophosphate Nanosheets Incorporated Nâ€doped Carbon for Efficient and Stable Electrocatalytic Water Splitting. Advanced Functional Materials, 2018, 28, 1805075.	14.9	57
67	Selfâ€Assemble and In Situ Formation of Ni _{1â^'} <i>_x<i>E<i>_x</i>PS₃ Nanomosaicâ€Decorated MXene Hybrids for Overall Water Splitting. Advanced Energy Materials, 2018, 8, 1801127.</i></i>	19.5	204
68	An <i>in situ</i> eutectic remelting and oxide replacement reaction for superior thermoelectric performance of InSb. Journal of Materials Chemistry A, 2018, 6, 17049-17056.	10.3	20
69	Low-Temperature Solution-Processed ZnSe Electron Transport Layer for Efficient Planar Perovskite Solar Cells with Negligible Hysteresis and Improved Photostability. ACS Nano, 2018, 12, 5605-5614.	14.6	89
70	Investigation on the microstructure and thermoelectric performance of magnetic ions doped Bi0.5Sb1.5Te3 solidified under a magnetostatic field. Acta Materialia, 2017, 127, 185-191.	7.9	15
71	New insight into InSb-based thermoelectric materials: from a divorced eutectic design to a remarkably high thermoelectric performance. Journal of Materials Chemistry A, 2017, 5, 5163-5170.	10.3	63
72	Multi-cations compound Cu2CoSnS4: DFT calculating, band engineering and thermoelectric performance regulation. Nano Energy, 2017, 36, 156-165.	16.0	47

#	Article	IF	CITATIONS
73	Synergistic effect by Na doping and S substitution for high thermoelectric performance of p-type MnTe. Journal of Materials Chemistry C, 2017, 5, 5076-5082.	5.5	40
74	Simultaneous regulation of electrical and thermal transport properties in CuInTe2 by directly incorporating excess ZnX (X=S, Se). Nano Energy, 2017, 32, 80-87.	16.0	44
75	Hexagonal-Phase Cobalt Monophosphosulfide for Highly Efficient Overall Water Splitting. ACS Nano, 2017, 11, 11031-11040.	14.6	297
76	Recent advances in printable secondary batteries. Journal of Materials Chemistry A, 2017, 5, 22442-22458.	10.3	50
77	Thermoelectric performance of SnTe with ZnO carrier compensation, energy filtering, and multiscale phonon scattering. Journal of the American Ceramic Society, 2017, 100, 5723-5730.	3.8	44
78	Combination of Carrier Concentration Regulation and High Band Degeneracy for Enhanced Thermoelectric Performance of Cu ₃ SbSe ₄ . ACS Applied Materials & Interfaces, 2017, 9, 28558-28565.	8.0	30
79	Feâ€Doped Ni ₃ C Nanodots in Nâ€Doped Carbon Nanosheets for Efficient Hydrogenâ€Evolution and Oxygenâ€Evolution Electrocatalysis. Angewandte Chemie, 2017, 129, 12740-12744.	2.0	48
80	Designing hybrid architectures for advanced thermoelectric materials. Materials Chemistry Frontiers, 2017, 1, 2457-2473.	5.9	34
81	Feâ€Doped Ni ₃ C Nanodots in Nâ€Doped Carbon Nanosheets for Efficient Hydrogenâ€Evolution and Oxygenâ€Evolution Electrocatalysis. Angewandte Chemie - International Edition, 2017, 56, 12566-12570.	13.8	324
82	General and Scalable Solidâ€ S tate Synthesis of 2D MPS ₃ (M = Fe, Co, Ni) Nanosheets and Tuning Their Li/Na Storage Properties. Small Methods, 2017, 1, 1700304.	8.6	90
83	Synergistic Effect to High-Performance Perovskite Solar Cells with Reduced Hysteresis and Improved Stability by the Introduction of Na-Treated TiO ₂ and Spraying-Deposited CuI as Transport Layers. ACS Applied Materials & Interfaces, 2017, 9, 41354-41362.	8.0	102
84	Simultaneous optimization of the overall thermoelectric properties of Cu3SbSe4 by band engineering and phonon blocking. Journal of Alloys and Compounds, 2017, 724, 597-602.	5.5	22
85	Enhanced photovoltaic performance and stability in mixed-cation perovskite solar cells via compositional modulation. Electrochimica Acta, 2017, 247, 460-467.	5.2	41
86	Carriers concentration tailoring and phonon scattering from n-type zinc oxide (ZnO) nanoinclusion in p- and n-type bismuth telluride (Bi2Te3): Leading to ultra low thermal conductivity and excellent thermoelectric properties. Journal of Alloys and Compounds, 2017, 694, 864-868.	5.5	26
87	Improvement of photovoltaic performance of perovskite solar cells with a ZnO/Zn2SnO4 composite compact layer. Solar Energy Materials and Solar Cells, 2017, 159, 143-150.	6.2	31
88	Thermal Stability of P-Type BiSbTe Alloys Prepared by Melt Spinning and Rapid Sintering. Materials, 2017, 10, 617.	2.9	18
89	Progressive Regulation of Electrical and Thermal Transport Properties to Highâ€Performance CulnTe ₂ Thermoelectric Materials. Advanced Energy Materials, 2016, 6, 1600007.	19.5	118
90	A new method for simultaneous measurement of Seebeck coefficient and resistivity. Review of Scientific Instruments, 2016, 87, 124901.	1.3	13

#	Article	IF	CITATIONS
91	Enhancement of photovoltaic performance of perovskite solar cells by modification of the interface between the perovskite and mesoporous TiO2 film. Solar Energy Materials and Solar Cells, 2016, 155, 101-107.	6.2	51
92	Effect of cooling rate on the thermoelectric and mechanical performance of Bi0.5Sb1.5Te3 prepared under a high magnetic field. Intermetallics, 2016, 72, 62-68.	3.9	9
93	Microstructure tailoring in nanostructured thermoelectric materials. Journal of Advanced Dielectrics, 2016, 06, 1630002.	2.4	24
94	Enhanced thermoelectric performance of MnTe via Cu doping with optimized carrier concentration. Journal of Materiomics, 2016, 2, 172-178.	5.7	24
95	Enhancement of thermoelectric properties of Ce0.9Fe3.75Ni0.25Sb12p-type skutterudite by tellurium addition. Journal of Materials Chemistry A, 2016, 4, 16499-16506.	10.3	13
96	Multiple effects of Bi doping in enhancing the thermoelectric properties of SnTe. Journal of Materials Chemistry A, 2016, 4, 13171-13175.	10.3	128
97	Preparation and Photovoltaic Properties of Ternary AgBiS ₂ Quantum Dots Sensitized TiO ₂ Nanorods Photoanodes by Electrochemical Atomic Layer Deposition. Journal of the Electrochemical Society, 2016, 163, D63-D67.	2.9	30
98	Large improvement of device performance by a synergistic effect of photovoltaics and thermoelectrics. Nano Energy, 2016, 22, 120-128.	16.0	30
99	Ternary CuSbSe ₂ chalcostibite: facile synthesis, electronic-structure and thermoelectric performance enhancement. Journal of Materials Chemistry A, 2016, 4, 4188-4193.	10.3	69
100	Electrochemical atomic layer deposition of Bi2S3/Sb2S3 quantum dots co-sensitized TiO2 nanorods solar cells. Journal of Power Sources, 2016, 307, 690-696.	7.8	47
101	Improvement of thermoelectric properties of Cu 3 SbSe 4 compound by In doping. Materials and Design, 2016, 98, 150-154.	7.0	62
102	Improvement of Thermoelectric Properties of Bi0.4Sb1.6Te3 with Addition of Nanoscale Zinc Oxide Particles. Journal of Electronic Materials, 2016, 45, 1266-1270.	2.2	17
103	Thermoelectric Performance Enhancement of CeFe4Sb12 p-Type Skutterudite by Disorder on the Sb4 Rings Induced by Te Doping and Nanopores. Journal of Electronic Materials, 2016, 45, 1240-1244.	2.2	12
104	Effect of TiC Nanoinclusions on Thermoelectric and Mechanical Performance of Polycrystalline In ₄ Se _{2.65} . Journal of the American Ceramic Society, 2015, 98, 3813-3817.	3.8	10
105	CuCrSe ₂ Ternary Chromium Chalcogenide: Facile Fabrication, Doping and Thermoelectric Properties. Journal of the American Ceramic Society, 2015, 98, 3975-3980.	3.8	19
106	Melting and solidification of bismuth antimony telluride under a high magnetic field: A new route to high thermoelectric performance. Nano Energy, 2015, 15, 709-718.	16.0	35
107	Fabrication of CdSe/CdTe Quantum Dots Co-Sensitized TiO ₂ Nanorods by Electrochemical Atomic Layer Deposition Method. Journal of the Electrochemical Society, 2015, 162, D137-D141.	2.9	6
108	Multi-role of Sodium Doping in BiCuSeO on High Thermoelectric Performance. Journal of Electronic Materials, 2015, 44, 2849-2855.	2.2	26

#	Article	IF	CITATIONS
109	Bi-layer of nanorods and three-dimensional hierarchical structure of TiO 2 for high efficiency dye-sensitized solar cells. Journal of Power Sources, 2015, 284, 428-434.	7.8	22
110	Synergistic tuning of carrier and phonon scattering for high performance of n-type Bi ₂ Te _{2.5} Se _{0.5} thermoelectric material. Journal of Materials Chemistry A, 2015, 3, 22332-22338.	10.3	25
111	Large enhancement of thermoelectric performance of CulnTe 2 via a synergistic strategy of point defects and microstructure engineering. Nano Energy, 2015, 18, 37-46.	16.0	78
112	Enhancement of thermoelectric properties of Yb-filled skutterudites by an Ni-Induced "core–shell― structure. Journal of Materials Chemistry A, 2015, 3, 1010-1016.	10.3	63
113	Multiple heteroatom induced carrier engineering and hierarchical nanostructures for high thermoelectric performance of polycrystalline In ₄ Se _{2.5} . Journal of Materials Chemistry A, 2015, 3, 1251-1257.	10.3	38
114	Fabrication of CdTe Quantum Dots Sensitized TiO ₂ Nanorod-Array-Film Photoanodes via the Route of Electrochemical Atomic Layer Deposition. Journal of the Electrochemical Society, 2014, 161, D55-D58.	2.9	27
115	A simultaneous increase in the ZT and the corresponding critical temperature of p-type Bi _{0.4} Sb _{1.6} Te ₃ by a combined strategy of dual nanoinclusions and carrier engineering. Journal of Materials Chemistry A, 2014, 2, 20288-20294.	10.3	35
116	Enhanced thermoelectric and mechanical performance of polycrystalline p-type Bi0.5Sb1.5Te3 by a traditional physical metallurgical strategy. Intermetallics, 2014, 50, 20-27.	3.9	25
117	Enhancement of the Thermoelectric Performance of Polycrystalline In ₄ Se _{2.5} by Copper Intercalation and Bromine Substitution. Advanced Energy Materials, 2014, 4, 1300599.	19.5	71
118	Enhanced photovoltaic performance of CdS quantum dots sensitized highly oriented two-end-opened TiO2 nanotubes array membrane. Journal of Power Sources, 2014, 250, 174-180.	7.8	20
119	Electrochemical Atomic Layer Deposition of Ag ₂ S Quantum Dots Sensitized TiO ₂ Nanorods Array Photoanodes and Cu ₂ S Counter Electrode for Solar Cells. Journal of the Electrochemical Society, 2014, 161, D510-D514.	2.9	14
120	A study of Yb _{0.2} Co ₄ Sb ₁₂ –AgSbTe ₂ nanocomposites: simultaneous enhancement of all three thermoelectric properties. Journal of Materials Chemistry A, 2014, 2, 73-79.	10.3	45
121	Improve photovoltaic performance of titanium dioxide nanorods based dye-sensitized solar cells by Ca-doping. Materials Research Bulletin, 2014, 57, 177-183.	5.2	34
122	AgSbTe2 nanoinclusion in Yb0.2Co4Sb12 for high performance thermoelectrics. Intermetallics, 2013, 43, 79-84.	3.9	17
123	Hierarchical double-layered SnO2 film as a photoanode for dye-sensitized solar cells. New Journal of Chemistry, 2013, 37, 1002.	2.8	8
124	Improvement of Thermoelectric Properties of <scp><scp>In</scp></scp> 4 <scp><scp>Se</scp></scp> ₃ Bulk Materials with Cu Nanoinclusions. Journal of the American Ceramic Society, 2013, 96, 2703-2705.	3.8	24
125	CdS quantum dots sensitized TiO2 nanorod-array-film photoelectrode on FTO substrate by electrochemical atomic layer epitaxy method. Electrochimica Acta, 2012, 83, 321-326.	5.2	32
126	Composite photoanodes of Zn2SnO4 nanoparticles modified SnO2 hierarchical microspheres for dye-sensitized solar cells. Materials Letters, 2012, 76, 215-218.	2.6	40

#	Article	IF	CITATIONS
127	Characterization and Thermoelectric Properties of La0.4Ni0.2Co3.8Sb12 Filled Skutterudite Prepared by the MA-HP Method. Journal of the American Ceramic Society, 2011, 94, 277-280.	3.8	4
128	Coaxial Heterogeneous Structure of TiO ₂ Nanotube Arrays with CdS as a Superthin Coating Synthesized via Modified Electrochemical Atomic Layer Deposition. Journal of the American Chemical Society, 2010, 132, 12619-12626.	13.7	159
129	Electrodeposition and characterization of Bi2Se3 thin films by electrochemical atomic layer epitaxy (ECALE). Electrochimica Acta, 2009, 54, 6821-6826.	5.2	39
130	Effect of processing parameters on formation and thermoelectric properties of La0.4FeCo3Sb12 skutterudite by MA–HP method. Journal of Alloys and Compounds, 2009, 476, 802-806.	5.5	15
131	Thermoelectric properties of silver-doped n-type Bi2Te3-based material prepared by mechanical alloying and subsequent hot pressing. Journal of Alloys and Compounds, 2006, 407, 330-333.	5.5	64
132	Preparation and thermoelectric properties of LaxFeCo3Sb12 skutterudites by mechanical alloying and hot pressing. Journal of Alloys and Compounds, 2006, 421, 105-108.	5.5	18
133	Effect of La filling on thermoelectric properties of LaxCo3.6Ni0.4Sb12-filled skutterudite prepared by MA–HP method. Journal of Solid State Chemistry, 2006, 179, 212-216.	2.9	19
134	Synthesis of CoSb3 skutterudite by mechanical alloying. Journal of Alloys and Compounds, 2004, 375, 229-232.	5.5	67
135	Preparation and characterization of Fe substituted CoSb3 skutterudite by mechanical alloying and annealing. Journal of Alloys and Compounds, 2004, 381, 313-316.	5.5	39
136	Study on mechanical alloying and subsequent heat treatment of the Ti–Si system. Physica B: Condensed Matter, 2000, 279, 241-245.	2.7	42